

An Automatic Framework for the Non-Rigid Alignment of Electroanatomical Maps and Preoperative Anatomical Scans in Atrial Fibrillation

Martino Alessandrini¹, Maddalena Valinoti¹, Antonio Pasini², Roberto Mantovan², Stefano Severi¹,
Cristiana Corsi¹

¹Department of Electrical, Electronic and Information Engineering, Università di Bologna, Cesena,
Italy

²Bufalini Hospital, Cesena, Italy.

Abstract

In atrial fibrillation, electro-anatomical maps (EAM) are used for ablation guidance. Yet, the anatomy reconstructed by the navigation system is known to be poorly accurate. This makes catheter navigation challenging and, as such, might affect ablation's outcome.

To ease navigation, existing systems allow co-registering EAMs with pre-operative MR scans by rigidly matching a set of manual landmarks. Nevertheless, the deformation between the two datasets is highly non-rigid.

The aim of this work was therefore to develop a framework for the non-rigid alignment of EAMs and anatomical scans to improve ablation guidance.

1. Introduction

Atrial fibrillation (AF) is the most common form of arrhythmia worldwide and entails substantial morbidity and mortality [1]. Due to the aging of the population and the better survival rates, the prevalence of AF is estimated at least to double in the next 50 years [1].

AF is often treated with minimally invasive catheter ablation since trials question the efficacy of pharmacological strategies [1]. Hereto, the so called electro-anatomical maps (EAMs) are used for procedure guidance [2]. EAMs integrate measured voltage maps on a reconstructed 3D atrial anatomy. Yet, the reconstructed anatomy has limited accuracy due to: 1) the intrinsic positioning errors of the navigation system; 2) the absence of time triggering, which implies that different parts in the geometry are likely to be acquired at different phases in the cardiac cycle. Overall, the absence of reliable anatomical information makes catheter ablation still challenging.

To ease navigation, modern systems allow importing pre-operative MR or CT scans, which are co-registered with the EAMs [3]. Hereto, the alignment is obtained by rigid matching between corresponding landmarks which are placed manually on both datasets.

Although integration with MR or CT is effective to improve ablation outcomes [3], rigid registration neglects the expectedly non-rigid deformation between the two datasets, as due to the aforementioned errors in the reconstructed EAMs anatomy, besides the fact that the two datasets are acquired in different patient's conditions.

The aim of this work was therefore to develop a framework for the non-rigid integration of EAMs and anatomical scans. Note that a conceptually similar effort in the context of ventricular ablation was presented in [4]. Yet, the techniques employed in our work are adapted to our intrinsically different clinical setting.

The paper proceeds as follows. Section 2 illustrates the methodology. Section 3 presents the evaluation metrics. Section 4 presents the results. Discussions and Conclusions are left to Section 5 and Section 6, respectively.

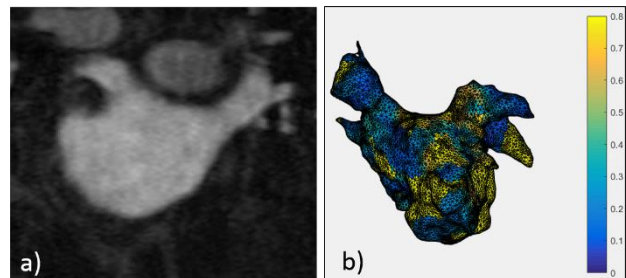


Figure 1. Clinical dataset: One coronal slice of one volumetric pre-operative MRA scan (a) and electro-anatomical map exported from the NavX system, where the measured surface potential is color-coded (b).

2. Materials and Methods

2.1. Evaluation dataset

We choose retrospectively data from 3 AF patients, enrolled for catheter ablation at the electrophysiology unit of the Bufalini Hospital, Cesena, Italy. Data included, for each patient, 1) one pre-operative magnetic resonance angiography (MRA) scan (average pixel spacing 0.7 x 0.7 mm, slice spacing 1.5 mm) and 2) one electro anatomical

map acquired during the ablation procedure (EnSite NavX, St. Jude Medical, St. Paul, MN, USA). The EAM was provided as a triangular surface mesh (cf. Fig. 2), which was extracted from the .xml files exported from the NavX system.

2.2. Left atrial segmentation from MRA

Left atrium and the initial tract of the pulmonary veins (PV's) were segmented from the MRA scan and used for successive alignment with the EAM mesh. Hereto, an automatic in-house technique was used, as previously described [5]. Briefly, Otsu thresholding was used to provide an initial mask. An analysis of size and position of each connected component, combined with a series of morphological operators, allowed to obtain a rough segmentation of the LA on each slice. Level-set [6] segmentation was used to refine the solution and regularize the contours. A surface triangular mesh was then extracted from the obtained binary mask by using iso2mesh [7], a MATLAB wrapping of the CGAL library [8].

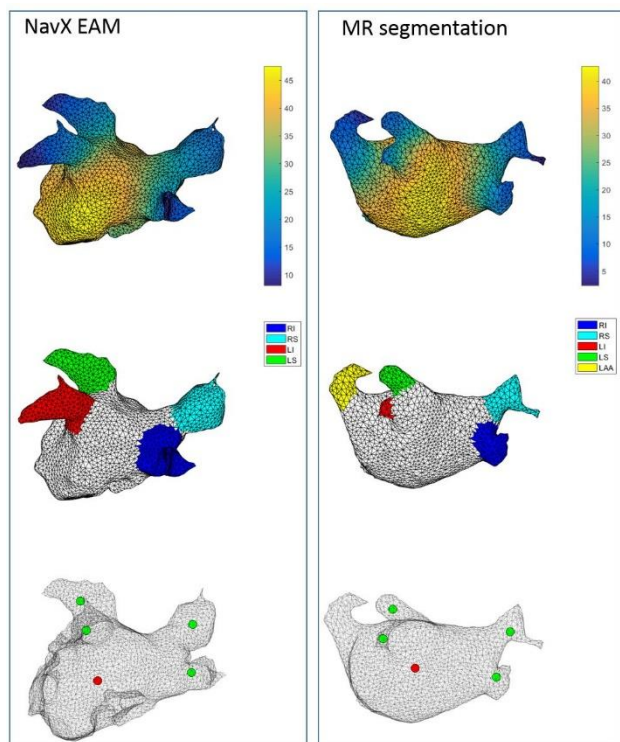


Figure 2: Top row: the input mesh where the shape diameter function is color coded on the facets. SDF values are in mm. Mid row: labelling of relevant anatomical structures based on the clustering of the SDF values. Note that the left atrial appendage, although detected, is not considered as a landmark (cf. text). The atrial body is painted in white. Bottom row: the 5 anatomical landmarks used for initial alignment (PVs in green, LA center in red). Left and right columns show the land-

marking process for EAM and MRA segmentation.

2.3. Automatic landmark detection

A set of 5 corresponding anatomical landmarks were automatically detected on both geometries, to be used for initial alignment as detailed later. These were the center of mass of the left atrial body plus the insertion point of the four pulmonary veins. The land-marking process is illustrated in Fig. 2.

The shape diameter function (SDF) of each triangular mesh was first computed [9]. The SDF measures, for each triangle, the local object diameter. Roughly, this is computed by casting rays inwards around the normal direction and detecting the closest intersecting triangle on the opposite side. As such, PV's and atrial body will have small and large SDF values, respectively (cf. Fig. 2, top).

A first partitioning of the meshes was then obtained by thresholding the SDF. Hereto, an initial threshold was obtained by clustering the SDF in two clusters by using the K-means algorithm. The threshold was then incrementally updated until the geometry was split into 5 connected components, roughly corresponding to the 5 anatomical regions of interest. The EAMs had a bumpy and irregular shape which resulted in the presence of small regions with low SDF in the LA region (cf. Fig. 1(b) and Fig. 2, left), which were incorrectly classified by the thresholding scheme. Those spurious regions were automatically detected based on size, shape and position and assigned to the LA body. Finally, the PV were expanded towards the LA body until a contact point was reached between PV's located on the same side (i.e. left and right). The anatomical position of each PV (i.e. left/right, superior/inferior) was assigned by using the information on the anatomical orientation contained in the headers of the exported files.

As such, each mesh was labeled into 5 anatomical regions (cf. Fig. 2, mid row). From the latter, the 5 landmark points were computed as follows: the insertion point of each PV was computed as the center of mass of the associated edge segments, while the fifth landmark was the center of mass of the LA (cf. Fig. 2, bottom).

2.4. Alignment

The two geometries were first aligned rigidly by using Procrustes analysis and the 5 anatomical landmarks as control points.

The transformation was then finalized by matching the full surfaces. Hereto, 5 techniques for point-cloud registration were contrasted. Iterative Closest Point (ICP) is a well-known solution for rigid alignment of point clouds when point-to-point correspondences are missing, as in our case. Coherent Point Drift (CPD) [10] was also used both to fit an affine transform (CPDaffine) and a

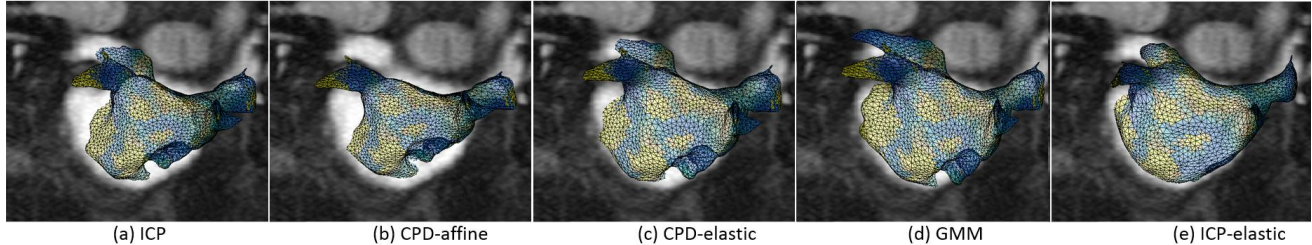


Figure 3: Example results obtained on one patient with each of the 5 considered techniques. The EAM after alignment is overlaid on the pre-operative MR scan.

non-rigid (i.e. elastic) transform (CPDelastic). The technique in [11], based on Generalized Gaussian Mixture Models (GMM) and a non-rigid version of the ICP algorithm (ICPelastic) [12] were also considered for non-rigid registration. CFD and GMM are similar in that they both start from a spatially continuous representation of the point sets represented as a Gaussian mixture model. This allows to define the point-matching problem as a statistical estimation problem, solved via expectation maximization. A detailed description of the techniques considered is unfeasible for brevity reasons.

3. Evaluation metrics

We applied our registration framework to align the EAM map on the segmented LA geometry (therefore, on the MRA scan). It is important to note that some of the differences between the two geometries might be anatomical differences coming, e.g., from the way pulmonary veins and left atrial appendage are cut. Those differences should not be cancelled out by the registration framework. Therefore, we aimed to achieve a meaningful balance between the goodness of match and the amount of distortion introduced. For the former we used Hausdorff distance (HD) and mean distance between (MD) the two meshes. Instead, to quantify how much the EAM has been deformed, we measured the MD between its original and its registered shape. Rigid transformations were removed before computing our deformation metric. HD and MD were measured in mm.

4. Results

The obtained results are summarized in Table 1. An example of the output of each technique is provided in Fig. 3. As compared to initial landmark based alignment, ICP implies a simple adjustment in the axes direction. Therefore, there is no significant change in the metrics considered. Note that the distortion introduced is zero because our definition of distortion does not account for roto-translations.

Table 1. HD and MD (in mm) between the two geometries (inter) and amount of distortion introduced. The first row corresponds to the landmark based pre-alignment.

	MD _{inter}	HD _{inter}	Distortion
INITIAL	4.47	15.44	0
ICP	4.36	16.50	0
CPD _{affine}	4.06	13.78	6.21
CPD _{elastic}	1.92	13.41	6.34
GMM	1.81	13.35	6.73
ICP _{elastic}	1.34	11.12	8.51

Affine matching reduced both HD and MD, nonetheless, visual inspection did not show a substantial improvement as compared to rigid ICP (cf. Fig. 3(b)). Non rigid CFD and GMM improved the alignment between the two modalities considerably (cf. Fig. 3), by keeping distortion close to the value obtained with an affine transform. Non rigid ICP achieved the best matching between the two modalities but implied the largest deformation.

5. Discussion

We have shown how elastic registration could be used to match pre-operative anatomical scans and intra-operative EAM in atrial fibrillation. Clearly, the most critical point is to achieve a meaningful balance between the goodness of match and the amount of deformation introduced. Hereto, in this paper we provided a very simple measurement of distortion. This should be improved in the future to include clinically meaningful quantities, e.g. anatomical landmarks. They could be also used as additional constraint to guide the non-rigid registration step. Dealing with these aspects is the topic of ongoing research.

From this exploratory study, it appeared that both CPD and GMM improved the matching by preserving the local morphology of the EAM. Non rigid ICP resulted in the best matching, but it seemed to inflate the EAM with the risk of matching anatomically different regions of tissue.

Although shown for MRA, the same framework could be applied to any image modality. In particular, late-enhancement MR has been shown to be appropriate to

map atrial scar and fibrosis, and there is compelling evidence of how such structural features impact electrical activation and explain fibrillation progression [13]. Our framework could therefore be used to study the correspondence between structural and electrical features more directly and objectively. This specific application is the object of our ongoing efforts.

Despite these limitations, this is to our knowledge the first study to evaluate the benefits of elastic registration to improve the correspondence between electrical activation and anatomical content in the context of atrial fibrillation.

6. Conclusions

We presented a framework to align the electroanatomical maps used during AF ablation onto pre-operative anatomical scans by using non-rigid registration.

As compared to standard rigid registration, the framework is shown promising in establishing a closer and therefore more objective correspondence between the two datasets. This could be helpful to ease catheter navigation during ablation. Moreover, it would allow studying more accurately the correspondence between specific fibrillatory patterns (e.g. reentries) and anatomical/structural features (e.g. atrial fibrosis).

Acknowledgements

This project has received funding from the European Union's Horizon 2020 research and innovation programme under the Marie Skłodowska-Curie grant agreement No 659082.

References

- [1] Camm AJ et al.: Guidelines for the management of atrial fibrillation Developed with the special contribution of the European Heart Rhythm Association (EHRA), Endorsed by the European Association for Cardio-Thoracic Surgery (EACTS), Authors/Task Force Members. *European Heart Journal* 2010;31(19):2369-2429.
- [2] Bhakta D, Miller JM. Principles of Electroanatomic Mapping. *Indian Pacing and Electrophysiology Journal*. 2008;8(1):32-50.
- [3] Heist EK, Chevalier J, Holmvang G. et al., Factors affecting error in integration of electroanatomic mapping with CT and MR imaging during catheter ablation of atrial fibrillation, *J Interv Card Electrophysiol* 2006;17:21.
- [4] Soto-Iglesias D, Butakoff C, Andreu D, Fernández-Armenta J, Berruezo A, Camara, O, *Functional Imaging and Modelling of the Heart*, 2013;7945:391–399.
- [5] Leonardi R, Veronesi F, Severi S, Mantovan R, Corsi C, Volumetric identification of left atrial fibrosis from delayed enhancement magnetic resonance imaging in atrial fibrillation: Preliminary results, *Computing in Cardiology* 2014, IEEE Press,41:101-104.
- [6] Malladi R, Sethian JA, Vemuri BC, Shape modeling with front propagation: a level set approach, in *IEEE Transactions on Pattern Analysis and Machine Intelligence* 1995;17(2):158-175.
- [7] Fang Q, Boas D, Tetrahedral mesh generation from volumetric binary and gray-scale images," *Proceedings of IEEE International Symposium on Biomedical Imaging* 2009;1142-1145.
- [8] <http://www.cgal.org/>
- [9] Shapira L, Shamir A, Cohen-Or D, Consistent mesh partitioning and skeletonisation using the shape diameter function. *The Visual Computer*, 2008;24(4):249–259.
- [10] Myronenko A, Song X, Point-Set Registration: Coherent Point Drift, *IEEE Trans. on Pattern Analysis and Machine Intelligence* 2010;32(12):2262-2275.
- [11] Jian B, Vemuri BC, Robust Point Set Registration Using Gaussian Mixture Models, *IEEE Transactions on Pattern Analysis and Machine Intelligence* 2011;33(8):1633-1645.
- [12] Amberg B, Romdhani S, Vetter T, Optimal step non rigid icp algorithms for surface registration, *CVPR* 2007.
- [13] Zahid, S, Cochet H, Boyle PM, Schwarz EL, Whyte KN, Vigmond EJ, Trayanova NA, Patient-derived models link reentrant driver localization in atrial fibrillation to fibrosis spatial pattern. *Cardiovascular Research*, 2016;110(3):443-54.

Address for correspondence:

Martino Alessandrini
Dipartimento di Ingegneria dell'Energia Elettrica e dell'Informazione, Università di Bologna
Viale Risorgimento, 2 - 40136, Bologna, Italy.
martino.alessandrini@unibo.it